

Style Variable and Irrelevant Learning for Generalizable Person Re-identification

Haobo Chen*, Chuyang Zhao*, Kai Tu, Junru Chen, Yadong Li, and Boxun Li

Abstract—Recently, due to the poor performance of supervised person re-identification (ReID) to an unseen domain, Domain Generalization (DG) person ReID has attracted a lot of attention which aims to learn a domain-insensitive model and can resist the influence of domain bias. In this paper, we first verify through an experiment that style factors are a vital part of domain bias. Base on this conclusion, we propose a Style Variable and Irrelevant Learning (SVIL) method to eliminate the effect of style factors on the model. Specifically, we design a Style Jitter Module (SJM) in SVIL. The SJM module can enrich the style diversity of the specific source domain and reduce the style differences of various source domains. This leads to the model focusing on identity-relevant information and being insensitive to the style changes. Besides, we organically combine the SJM module with a meta-learning algorithm, maximizing the benefits and further improving the generalization ability of the model. Note that our SJM module is plug-and-play and inference cost-free. Extensive experiments confirm the effectiveness of our SVIL and our method outperforms the state-of-the-art methods on DG-ReID benchmarks by a large margin.

Index Terms—Person re-identification, Domain generalization, Style variable, Meta-learning.

I. INTRODUCTION

Person re-identification (ReID) aims to identify a specific person across non-overlapping cameras under various views and scenes. It has attracted a lot of attention due to its significance to intelligent surveillance systems. With the development of deep learning techniques, person ReID has achieved remarkable performance in supervised manner, where a model is trained and tested on the same dataset [1]–[7]. Unfortunately, due to the dramatic domain bias, these ReID models suffer from severe performance degradation when applying to an unseen domain. To cope with this issue, tasks of unsupervised domain adaption (UDA) and domain generalization ReID (DG-ReID) have attracted lots of attention in recent years. In UDA task, the images of target domains are available but these labels are unknown. These approaches [8]–[11] generally adapt the source-trained model and utilize the unlabeled target data to finetune. Whereas in DG-ReID, both images and labels are invisible, which makes the task more challenging but practical.

Existing DG-ReID methods can be roughly divided into three main aspects. Adversarial learning based methods [12],

Haobo Chen and Chuyang Zhao ({hbchen121, cy.zhao15}@gmail.com) have the equal contribution, and this work was done when they were interns at MEGVII Technology.

Kai Tu, Junru Chen, Yadong Li and Boxun Li are all algorithm research engineers of MEGVII Technology ({tukai, chenjunru, liyadong, liboxun}@megvii.com). Corresponding author: Yadong Li.

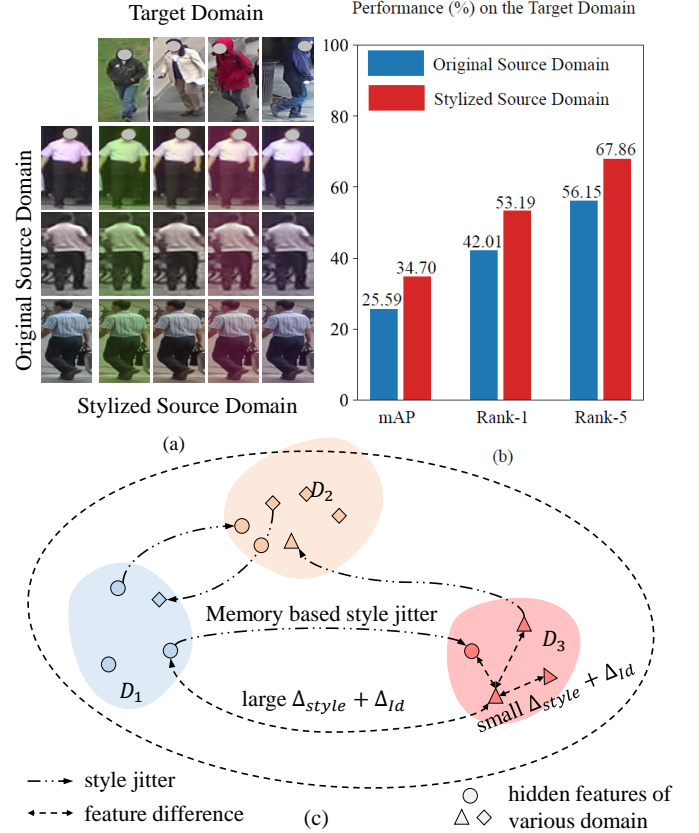


Fig. 1. Illustration of experiments exploring the influence of style factors in domains bias. (a) The exploratory experiment introduces the style information of the target domain into the original source domain and then obtain the stylized source domain. (b) The experiments results of the model trained on original/stylized source domain and tested on the target domain. The performance is obviously improved after introducing style information. (c) The visualization of hidden features affected by style jitter module.

[13] employ the adversarial auto-encoder module and discrimination task to help extract domain-invariant features, but these methods may fall into the unbalanced training between several tasks. Normalization based methods [14]–[16] utilize the instance normalization (IN) to disentangle the identity-relevant and identity-irrelevant features. They generally focus on a single sample and ignore the relationship between multiple samples, including intra-domain and inter-domain. Meta-learning based methods [17]–[19] split the train datasets into meta-train and meta-test to simulate the domain bias, adopting a process of “learning-to-learn” to optimize the model. Although the goal of meta-learning is to prevent the model from overfitting, as the training process progresses, the model

will witness enough data (including the data in the meta-test) and then inevitably fall into overfitting. Most of methods mentioned above are inspired by approaches in conventional DG task, which is a classification task and different from DG-ReID task. Specifically, researchers typically define various datasets as different domains. The datasets (domains) in conventional DG task may contains real image dataset and painting picture dataset, where the domain bias is obvious. However, DG-ReID task involves only real image datasets. Images in different datasets (domains) are captured from different cameras and regions.

In this paper, we consider a basic problem: “what factors does domain bias contain in DG-ReID?” An intuitive idea is that the domain bias (*i.e.*, the differences between various datasets) may include scene, season, camera angle and style (*e.g.* illumination and hue). To explore the influence of style factors in domain bias, we conduct a simple exploratory experiment as illustrated in Fig. 1. Specifically, by replacing the mean and variance statistics of the images, in Fig. 1 (a) we introduce the style information of the target domain (DukeMTMC [20]) into the source domain (Market 1501 [21]), where the mean and variance are considered and proved as style representation in the transfer learning task [22]–[24]. The results in Fig. 1 (b) shows that we can achieve better ReID performance by training on the source domain with the same style as the target domain, confirming that the style factors are a vital part of domain bias. However, style information of the target domain is unavailable in DG-ReID. This makes us have to eliminate the influence of style factors to reduce the domain bias.

Inspired by the above observations, we propose a Style Variable and Irrelevant Learning (SVIL) method for DG-ReID. We start our approach with multi-source DG-ReID task. Different with multi-source DG classification task, the label spaces of various source domains in DG-ReID are different. This means that an identity exists only in its specific domain, and identity and domain are strongly related. As shown in Fig. 1 (c), identity x_1^a belongs to domain D_1 , and identities x_3^b and x_3^c belongs to domain D_3 . Here we do not consider the influence of non-style domain bias and there are large style difference between cross-domain identities (*e.g.*, x_1^a and x_3^b). Then models can easily distinguish these identities relying on the style bias, thereby ignoring the extraction of identity information and achieving poor generalization. To prompt the model focusing on identity-relevant information and be insensitive to the style variations, our SVIL enhance the style diversity of the specific source domain and reducing the style differences of different source domains. More concretely, we design a Style Jitter Module (SJM) to enrich the style diversity of source domains. The SJM module uses style memory to store identity style statistics in all source domains. Then for each identity in mini-batch, we generate a new style statistic based on all statistics, where the new style is a weighting of the negative sample styles in all domains based on the identity relationship modeling. The original style is replace by the new style to destroy the relationship between original style and identity. To better distinguish hard negative samples, we strengthen the importance of the styles of hard samples

during style generation by hard identity emphasis. Besides, we perform cross-domain identity emphasis strategy to avoid the information of identities within the same domain to dominate the generated styles. Our SJM module is a inference cost-free module, without learnable parameters. It leads to variable styles between training samples and makes negative samples harder.

In addition, we notice that previous methods [14], [25], [26] employ a unified loss functions on multiple domains to learning feature representations. They omit the strong relationship between identity and domain caused by various label spaces. To weaken the relationship, we propose domain-agnostic loss and domain-specific loss to jointly learn robust features. A meta collaborative training procedure is employed as well to maximize the effectiveness of our SJM module, where the meta-learning algorithm is organically combined. The SJM module can enlarge and continuously change the domain bias between meta-train and meta-test, successfully delaying the model from overfitting. The combination of these two sub-method produce a synergy effect, leading to a style-irrelevant model to generalize to the unseen target domain.

We also perform the proposed SVIL on the single-source DG-ReID task to confirm its effectiveness. Specifically, because images captured under different cameras have stylistic differences, we divide a single dataset into multiple sub-datasets according to cameras. Then we employ SVIL on the single-source DG-ReID task to learn style-insensitive model as we do on the multi-source DG-ReID task. In summary, the major contributions of our works are summarized as follows:

- Based on the observation that style factors play a vital role in DG-ReID, we propose a Style Variable and Irrelevant Learning (SVIL) method to eliminate the influence of style variations and ah.
- We propose a Style Jitter Module (SJM) to generate diverse styles for identities, increasing the variety of feature styles. It forces the model to focus on identity-relevant information and ignore style-relevant information.
- We apply a meta collaborative training procedure to get rid of the influence of style further. Our approach outperforms state-of-the-art methods by a large margin in both multi-source and single-source DG-ReID tasks.

The rest of this paper is organized as follows. Section II reviews and discusses the related works. Section III first introduce s the overall framework of the proposed method, and then elaborate the designed style jitter module and the training procedure. Section IV presents the experimental results. Finally, Section V draws the conclusion.

II. RELATED WORKS

Re-identification. Re-identification (ReID) tasks have attracted a lot of attention due to their wide application in urban surveillance and intelligent transportation [27], [28]. Both person ReID and vehicle ReID have achieved significant performance through supervised learning approaches. For instance, Sun *et al.* [1] propose a circle loss function for deep feature learning. Chu *et al.* [2] propose a novel viewpoint-aware metric learning approach for vehicle Re-ID. He *et al.*

[3] design a pure transformer framework to ReID tasks and achieve remarkable performance. Other various attempts [4]–[7] along supervised learning acquire great performance as well. However, all of them pay little attention to exploring invariant information across domains, which limits their effects in practical applications. Therefore, Unsupervised Domain Adaptation (UDA) methods [8]–[11] are proposed to alleviate differences between the source domain and target domain. For instance, Ge *et al.* [8] propose a MMT framework to tackle the noise label in clustering process. Song *et al.* [9] employ a self-training scheme to iteratively minimize the loss functions. These methods require enough unlabeled training data of target domain, which is unsatisfactory in many practical situations. Then the domain generalization task is established.

Domain Generalization. The goal of Domain Generalization (DG) is to learn a model that is generalizable to unseen domains, having received more and more attention from the research community [24], [29], [30]. These methods generally assume that the source and target domains have the same label space. Whereas in DG-ReID, the label spaces are non-overlap. This results in methods in conventional DG can not be applied directly to DG-ReID. Adversarial learning is a popular method [12], [13] used in DG-ReID. For instance, Lin *et al.* [12] propose a multi-dataset feature generalization network to learning a universal domain-invariant feature representation and generalize it to unseen camera systems. Normalization-based method is also a mainstream solution in DG-ReID. For instance, Jin *et al.* [14] design a Style Normalization and Restitution (SNR) module to enhance generalization capabilities of networks. Choi *et al.* [15] propose the MetaBIN framework which prevents models from overfitting to the given source styles and improves the generalization capability to unseen domains. Compared to these methods, our SVIL can focus on more detailed style information. Beside, Model-Agnostic Meta-Learning (MAML) [17] is another popular method for DG-ReID. Zhao *et al.* [25] propose a memory-based framework to solve DG-ReID, where the meta-learning algorithm is adopted. Similarly, Dai *et al.* [26] also employ a vote experts under the meta-learning framework. In our method, the SJM module can contribute to the strengths of meta-learning, produce a synergy effect.

Style Transfer. In the field of style transfer, it has been proved that the statistical information of the features extracted by DNN can represent the style of the image [31]–[33]. Gatys *et al.* [31] use second-order statistical features as the optimization goal to achieve style transfer. Li *et al.* [33] find that other statistics (*i.e.*, mean and variance) of Batch Normalization (BN) layers contain the traits of different domains. Ulyanov *et al.* [34] utilize Instance Normalization (IN) to obtain the statistical characteristics of features. Dumoulin *et al.* [35] proposed Conditional Instance Normalization (CIN), which would learn pairs of α and β parameters during training. When both image content and decoding network are the same, adopting different pairs of α and β will get different styles of transfer results. In IN and CIN, the network can learn the affine transformation parameters α and β . In addition, to remove the two learnable parameters, AdaIN [22] are proposed. It directly replaces the two parameters with the mean and standard

deviation of the style image features.

III. METHOD

This purpose of our method is to narrow the domain gap caused by style variations in different domains. By increasing the style diversity on the training stage, the network will be insensitive to style changes between different domains and pay more attention to identity-relevant information. In this way, we can obtain a more generalizable model that can be deployed directly to a new unseen domain.

A. Overview

The main pipeline of our method is illustrated in Fig. 2 (a). In the train stage, we can access K source domains $\mathcal{D} = \{\mathcal{D}_k\}_{k=1}^K$, where $\mathcal{D}_k = \{(x_i^k, y_i^k)\}_{i=1}^{N_k}$ and (x_i^k, y_i^k) is a image-label pairs belong to \mathcal{D}_k , N_k is the number of images in the source domain \mathcal{D}_k . For each sample x_i^k , its label y_i^k comes from the specific label space \mathcal{Y}_k . By combining all source domains (termed global domain), we can obtain its global label $y_i^g \in \mathcal{Y}_g$, where \mathcal{Y}_g is the global label space. We sample B images x_i^k from each domain \mathcal{D}_k , where $B = \mathcal{P} \cdot \mathcal{K}$, meaning \mathcal{K} images from each of \mathcal{P} person identities. Then all images form a mini-batch of size $B \cdot K$ for all domains ($\mathcal{P} \cdot K$ identities in total). They are fed into the backbone network $f(\cdot)$ (*e.g.*, ResNet-50). After the Global Average Pooling (GAP), we design K domain-specific classifiers $\varphi_k(\cdot)$ and a domain agnostic classifier $\varphi_g(\cdot)$ to learn the feature representations.

We plugged the SJM module between stage-1 and stage-2. During the training phase, one half of the images of each identity pass through the SJM module, and the style information of feature representations in stage-1 is changed. The style of the other half of the images remain as it as, where the style information of different feature representations is changed. Next, all of the features are fed into stage-2 until the end of the network. We enforce domain-specific loss $\mathcal{L}_{\text{spec}}$ on each specific domains' features and predictions. To make the model more domain-insensitive, a domain-agnostic loss $\mathcal{L}_{\text{agno}}$ is employed on the global domains' features and predictions as well. Two losses jointly prompt the network to ignore the style variation of features and focus on identity-relevant information. In addition, we apply a meta-learning algorithm combined with the proposed SJM module to training the network, which can produce a synergy effect to our method (more details in Sec. III-D). Our SJM module is only used for training and will be discarded in testing.

B. Style Jitter Module

Images of different domains in DG ReID are generally captured from different cameras and scenes, leading to various styles. To address the style variations in DG ReID, we propose a SJM module to decreases the model's sensitivity to style variations. The SJM module takes one hidden representation from a specific domain as the input and generate a stylized representation, in which the cross-domain style information is transferred.

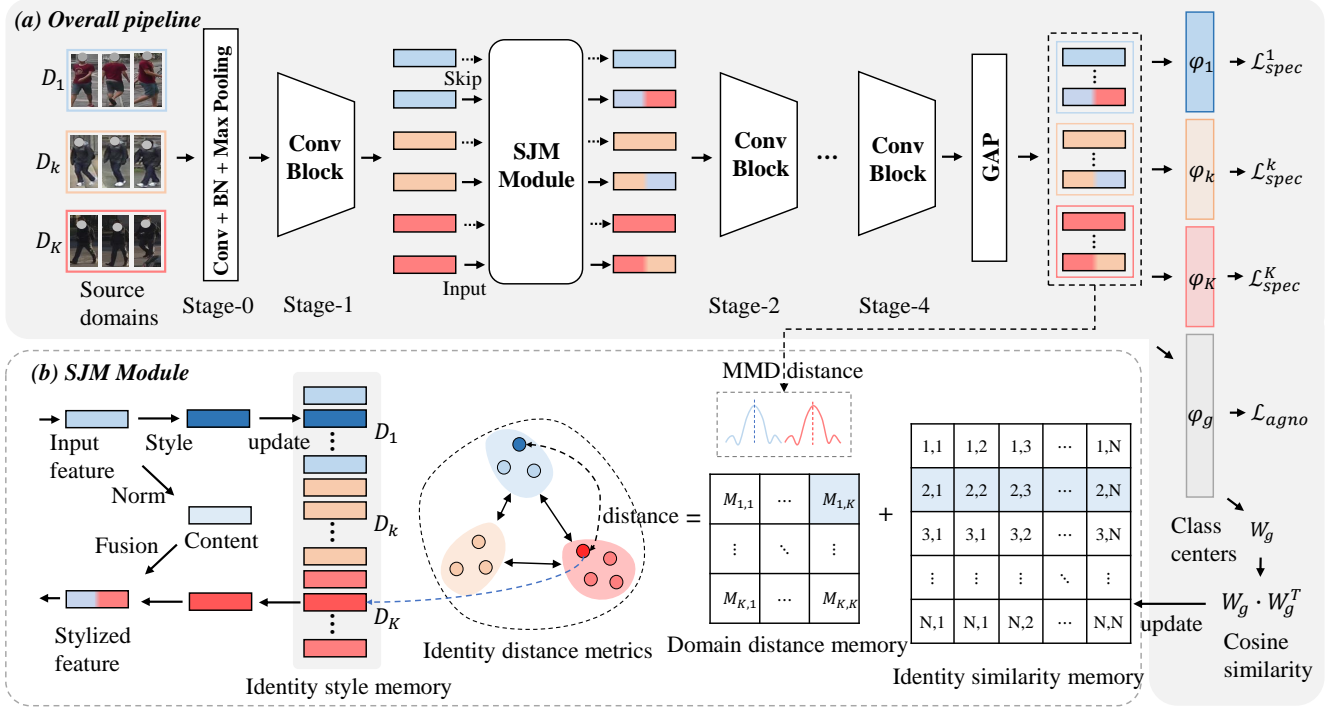


Fig. 2. Illustration of our method. (a) The overall pipeline of our method. The proposed SJM module can be plugged after any stage of the backbone (e.g., ResNet50), and we illustrate the structure of SJM between stage-1 and stage-2. In the training stage, we sample images from K source domains and group them into a mini-batch. Then images are fed into the backbone network and pass through the SRJ module, in which the style of features are changed within and across domains with the help of a style bank. After the Global Average Pooling (GAP), stylized features are utilized to calculate losses. Features from the same domain in the mini-batch are applied the same domain-specific loss \mathcal{L}_{spec} . All of the features calculate the domain-agnostic loss \mathcal{L}_{agno} .

Specifically, we denote backbone network as $f(x) = f_m(g_m(x))$, where g_m denotes the part of the network mapping the input data x to the hidden representation $F = g_m(x) \in \mathbb{R}^{H \times W \times C}$ after the m -th stage (e.g., $m = 1$ in Fig 2) and f_m denotes the part of the network mapping the feature $g_m(x)$ to the feature vector after the GAP layer. In a mini-batch including $\mathcal{P} \cdot K$ identities and each identity including \mathcal{K} images, we can obtain their maps at m -th hidden stage. For each identity, we select $\frac{\mathcal{K}}{2}$ representations F and diverse them by SJM module. As shown in Fig. 2 (b), we first compute the channel-wise mean and standard deviation $\mu(F), \sigma(F) \in \mathbb{R}^C$ by the style operation as follows:

$$\mu(F) = \frac{1}{HW} \sum_{h=1}^H \sum_{w=1}^W F_{hw}, \quad (1)$$

$$\sigma(F) = \sqrt{\frac{1}{HW} \sum_{h=1}^H \sum_{w=1}^W (F_{hw} - \mu(F))^2 + \epsilon}, \quad (2)$$

These feature statistics can capture informative characteristics of the specific domain and be viewed as style representation according to previous works [22]. Then we construct an identity style memory to store the style representations of each identity, where the cross-domain style representations are generated.

1) *Identity Style Memory Construction*: The style memory maintains the style representation of all identities. For $|\mathcal{Y}_g|$ identities from all source domains, the memory $\bar{\mathcal{M}}$ has $|\mathcal{Y}_g|$

slots, where each slot saves the style features of the corresponding identity. In initialization, we utilize the model to extract style representations for all source samples. Then we initialize the representation $\bar{\mathcal{M}}[j] = (\bar{\mu}[j], \bar{\sigma}[j])$ in memory using the average of all representations for j -th identity. At each training iteration, we update the memory with the style representations in the current mini-batch, which is formulated as:

$$\bar{\mu}[j] \leftarrow m \cdot \bar{\mu}[j] + (1 - m) \cdot \frac{2}{|\mathcal{B}_j|} \sum_{x_i \in \mathcal{B}_j} \mu(g_m(x_i)), \quad (3)$$

$$\bar{\sigma}[j] \leftarrow m \cdot \bar{\sigma}[j] + (1 - m) \cdot \frac{2}{|\mathcal{B}_j|} \sum_{x_i \in \mathcal{B}_j} \sigma(g_m(x_i)), \quad (4)$$

where $g_m(x_i)$ is the input feature F , \mathcal{B}_j refers to the samples belonging to the j -th identity and $|\mathcal{B}_j| = \mathcal{K}$ is the number of samples for the j -th identity in the current mini-batch. $m \in [0, 1]$ determines the update rate.

2) *Stylized Feature Generation*: To introduce information from other domains into the current specific domain, we generate new style representations by weighting all identity styles except the identities to which the input features belong. More concretely, we obtain an identity-related weight $\alpha \in \mathbb{R}^{|\mathcal{Y}_g|}$ for the input feature by identity relationship modelling (more detail in Sec. III-C). Then the new style representation is achieved by weighted fusion of the features of all identities as follows:

$$\mu' = \sum_{j=1}^{|\mathcal{Y}_g|} \alpha_j \bar{\mu}[j], \quad (5)$$

$$\sigma' = \sum_{j=1}^{|\mathcal{Y}_g|} \alpha_j \bar{\sigma}[j], \quad (6)$$

where $\bar{\mu}$ and $\bar{\sigma}$ are style representations in memory. Then we replace the style representation with the synthetic one to achieve the domain-agnostic feature, with is formulated as:

$$F' = \underbrace{\sum_{j=1}^{|\mathcal{Y}_g|} \alpha_j \bar{\sigma}[j]}_{\sigma'} \left(\frac{F - \mu(F)}{\sigma(F)} \right) + \sum_{j=1}^{|\mathcal{Y}_g|} \underbrace{\alpha_j \bar{\mu}[j]}_{\mu'}. \quad (7)$$

C. Identity Relationship Modeling

The identity-related weights control synthetic style representations and influence stylized features. Intuitively, for the features of a specific domain \mathcal{D}_k , on the one hand, we expect the generated features to contain more style information of other domains $\mathcal{D}_{i, i \neq k}$, which is conducive to learning domain-independent information. On the other hand, the synthesized features should be as difficult as possible, which is beneficial to improve the generalization ability of the model.

1) *Hard Identity Emphasis*: We obtain difficult synthetic features by emphasizing the stylistic features of hard identities, *i.e.*, larger identity-related weight α . As shown in Fig. 2 (a), we employ a domain-agnostic classifier $\varphi_g(\cdot)$ to classify all features in a mini-batch, where the domain-agnostic loss is adopted as follows:

$$\mathcal{L}_{agno} = \frac{1}{K} \sum_{k=1}^K \frac{1}{B} \sum_{i=1}^B \mathcal{L}_{ce}(\varphi_g(f(x_i^k)), y_i^g) + \mathcal{L}_{tri}(f(x), y^g), \quad (8)$$

where \mathcal{L}_{ce} denotes the cross-entropy loss and \mathcal{L}_{tri} denotes the triplet loss [36]. We normalize the weight W in $\varphi_g(\cdot)$ and the feature vectors $f(x)$, then the cross-entropy loss becomes as follow:

$$\mathcal{L}_{ce} = -\log \frac{\exp(\cos(W_{y_i^g}, f(x_i^k))/\tau)}{\sum_{j=1}^{|\mathcal{Y}_g|} \exp(\cos(W_j, f(x_i^k))/\tau)}, \quad (9)$$

in which $\cos(W_j, f(x)) = \frac{W_j^T \cdot f(x)}{\|W_j\| \cdot \|f(x)\|}$ is the cosine similarity between W_j and $f(x)$, τ is a temperature learnable parameter. Previous study [37] shows that the normalized weight W_j can be viewed as the center of features belonging to identity j . Inspired by this, we use the similarity between identity centers to represent the similarity between identities, which is calculated as follows:

$$S = \frac{W \cdot W^T}{\|W\| \cdot \|W\|} \quad (10)$$

where $S \in \mathbb{R}^{|\mathcal{Y}_g| \times |\mathcal{Y}_g|}$ and $S_{i,j}$ denotes the cosine similarity between identities i and j . Then we can calculate the identity-related weight based on identity similarities.

Identity Similarity Memory. At each training iteration, we cannot directly obtain the identity similarities of the current iteration in the SJM module. Therefore we use the historical cumulative similarity to calculate the weight, which brings the

added benefit that cumulative similarity is more representative of true identity similarity than current similarity. More concretely, we build a identity similarity memory \bar{S} to store the historical similarity via momentum updates. At initialization, we set $\bar{S}[j] = (\frac{1}{|\mathcal{Y}_g|}, \dots, \frac{1}{|\mathcal{Y}_g|})$ to treat all identities equally and $\bar{S}[j][j] = 0$ to avoid the influence of identity itself.

Then for each input feature whose identity is j , we can obtain the soft identity-related weight based on the similarity memory as follows:

$$\alpha = \text{softmax}(\beta), \quad (11)$$

where $\beta = \bar{S}[j]$ is the identity-related factor. The identity with high similarity to identity j (*i.e.*, the hard identity) has greater value, and its style representation are paid more attention. We can also focus only on the hardest identity by using the hard weight:

$$\alpha_i = \begin{cases} 1, & i = \arg \max_k(\beta) \\ 0, & i \neq \arg \max_k(\beta) \end{cases}, \quad (12)$$

where the hard weight $\alpha \in \mathbb{R}^{|\mathcal{Y}_g|}$ is a one-hot vector.

According to the weight we can get the generated stylized features as described in Sec III-B. All features in mini-batch are utilized to calculate the losses and update the network via gradient descent, including the weights W in $\varphi_g(\cdot)$. Then for each identity j , we set $S_{j,j} = 0$ and update the identity similarity memory:

$$\bar{S}[j] \leftarrow m \cdot \bar{S}[j] + (1 - m) \cdot S_j, \quad (13)$$

in which S is calculated by the last updated weight W .

2) *Cross-domain Identity Emphasis*: Although identity emphasis can make difficult identities get more attention, most of the difficult identities exist in the same domain, hindering the transfer of cross-domain information. To emphasis the cross-domain identities, we consider the influence of different domains when calculating identity-related weights, *i.e.*, give the cross-domain identities greater weights.

More specifically, we further introduce the relation (distances) between different domains when computing the identity-related factor β . As shown in Fig. 2 (a), a feature set $A_k = \{f(x_i^k)\}_{i=1}^B$ can be obtained for each source domain \mathcal{D}_k . Because the feature set A_k contains only a few features and is a subset of the domain \mathcal{D}_k , its distribution cannot represent the distribution of the entire domain. We model the distance between domains using the cumulative distribution distance between feature sets. Similar to identity similarity saving, we construct a domain distance memory \bar{D} to store the cumulative MMD distances between various feature sets. At each iteration, the distance between two sets is computed as follows:

$$D_{s,t} = \text{MMD}^2(A_s, A_t) = \left\| \frac{1}{|A_s|} \sum_{i=1}^B \phi(f(x_i^s)) - \frac{1}{|A_t|} \sum_{i=1}^B \phi(f(x_i^t)) \right\|^2, \quad (14)$$

where $\phi(\cdot)$ is a particular representation that maps the feature $f(x)$ into a reproducing kernel Hilbert space. The memory \bar{D} for k -th domain is updated as follows:

$$\bar{D}[k] \leftarrow m \cdot \bar{D}[k] + (1 - m) \cdot D_k. \quad (15)$$

Given the identity j of domain \mathcal{D}_k , we denote it as $\mathcal{D}^{-1}(j) = k$. To enhance the cross-domain identities, the identity-related factor β in Eq. 11 and Eq. 12 are redefined as follows:

$$\beta_i = \bar{S}[j][i] + \bar{D}[\mathcal{D}^{-1}(j)][\mathcal{D}^{-1}(i)], \quad (16)$$

where $\beta \in \mathbb{R}^{|\mathcal{D}_g|}$. In this way, information about difficult identities and information about cross-domain identities are simultaneously emphasized.

D. Training Procedure

To make the model focus on domain-independent identity information, we adopt two losses with different effect scopes to supervise the learning of the network. Furthermore, a Model-Agnostic Meta Learning (MAML) algorithm is applied to the training to maximize the effect of the proposed SJM module.

1) *Loss Functions: Domain-agnostic Loss.* Following the works [25] in conventional multi-source DG task, we employ a domain-agnostic loss (Eq. 8) whose effect scopes are all source domains, *i.e.*, global effect. More concretely, global influence refers to given an anchor sample x , its negative samples may come from any domain. By increasing the distance between pairs of negative samples, the model can learn the differences between them. However, because the identity and domain in DG person reid are highly correlated, the model can easily distinguish the features of different domains through focusing on domain bias. This makes the model ignore identity-related domain-independent information and reduces its generalization ability. Our SJM module exchanges style information across domains, allowing the model to focus on identity-related information. In addition, we use a domain-specific loss to reduce the model’s attention to domain-related information.

Domain-specific Loss. Different from domain-agnostic loss, the effect scopes of domain-specific loss is a specific domain. The specific loss for domain \mathcal{D}_k is formulated as follows:

$$\mathcal{L}_{spec}^k = \frac{1}{B} \sum_{i=1}^B \mathcal{L}_{ce}(\varphi_k(f(x_i^k)), y_i^k) + \mathcal{L}_{tri}(f(x^k), y^k). \quad (17)$$

Then the overall specific loss is as follows:

$$\mathcal{L}_{spec} = \frac{1}{K} \sum_{k=1}^K \mathcal{L}_{spec}^k. \quad (18)$$

It means that the anchor sample and its negative sample must belong to the same domain, *i.e.*, local effect. Then model are not affected by domain bias and focus on the domain-irrelevant information. In addition, SJM brings more styles to the features in the same domain. More hard samples are generated, and the model becomes more discriminative. Finally, the overall training loss is:

$$\mathcal{L}_{all} = \lambda \mathcal{L}_{agno} + (1 - \lambda) \mathcal{L}_{spec}, \quad (19)$$

2) *Meta Optimizing:* To maximize the effectiveness of the SJM module, we apply a Model-Agnostic Meta Learning (MAML) algorithm to our approach. The MAML adopts the concept of "learning-to-learn". It splits the source domains into meta-train and meta-test to simulate the domain bias, so as to improve the model generalization. Our SJM module can enlarge the domain bias by enriching the style diversity of meta-train, making the learning process of learning-to-learn harder and further improving the model generalization.

Specifically, we random split the K source domains into $K - 1$ meta-train domains and 1 meta-test domain. In the meta-train stage, the images are sampled from meta-train domains and grouped into a mini-batch, denoted as \mathcal{X}_S . Same as the previous training process, we fed these images into the network with the SJM module $f_S(\cdot; \Theta)$. We can calculate the meta-train loss \mathcal{L}_{mtr} (as same as \mathcal{L}_{all}) based on the stylized changed features. The gradient with respect to the meta-train loss is $\nabla_{\Theta} \mathcal{L}_{mtr}(f_S(\mathcal{X}_S; \Theta))$. Then we optimize the network and achieve an extra updated network:

$$\mathcal{L}_{all} = \lambda \mathcal{L}_{agno} + (1 - \lambda) \mathcal{L}_{spec}, \quad (20)$$

where λ denote the learning rate of meta-train optimizer. In the meta-test stage, we sample images from the meta-test domain and from a mini-batch, denoted as \mathcal{X}_T . Features in meta-test stage are produced by the updated network $f(\cdot; \Theta')$, where the SJM module is discarded. The meta-test loss \mathcal{L}_{mte} is calculated as well, in which \mathcal{L}_{mte} is the same as \mathcal{L}_{agno} because the specific-domain loss in \mathcal{L}_{all} is the same as \mathcal{L}_{agno} when there exists only one domain. Finally, we utilize the combination of the meta-train and meta-test losses to optimize the original model as follows:

$$\Theta \leftarrow \Theta - \gamma(\nabla_{\Theta} \mathcal{L}_{mtr}(f_S(\mathcal{X}_S; \Theta)) + \beta \nabla_{\Theta} \mathcal{L}_{mte}(f(\mathcal{X}_T; \Theta'))), \quad (21)$$

where γ is the learning rate of meta-test optimizer and β is the hyper-parameter to balance the gradient of the meta-train and meta-test losses. The overall training procedure of MAML is illustrated in Algorithm 1.

We randomly stylize images in meta-train domains and keep images in meta-test domains unchanged to mimic real train/test scenario. The intuition behind MAML is to expose the model to domain shift during training in hope that the model can avoid overfitting to source domain bias. In conventional methods of applying MAML directly to the meta-train/test domain, the domain bias between meta-train/test domains will gradually decrease after the model witnesses more and more training data in the iterative process. Whereas, our SJM module can alleviate this drawback. More concretely, the style of features in meta-train are jittered at each iteration and the style of features in meta-test are unchanged which makes the domain gap between meta-train and meta-test domains harder to fit. To learn a more generalizable model, the model has to ignore the influence of style variations between meta-train/test domains, and pay more attention to the identity-relevant information.

Algorithm 1: Training Procedure

Input: Source domains $\mathcal{D} = \{\mathcal{D}_k\}_{k=1}^K$; Learning rate hyperparameters α, β, γ .

Output: Model with the SJM module $f_S(\cdot; \Theta)$; Model w/o the SJM module $f(\cdot; \Theta)$; Domain-specific classifiers $\{\varphi_k(\cdot; W_k)\}_{k=1}^K$; Domain-agnostic classifier $\varphi_g(\cdot; W_g)$.

1 **Initialization:** Identity style memory $\bar{\mathcal{M}}$; Identity similarity memory \bar{S} ; Domain distance memory \bar{D} .

2 **for** *iter in iterations* **do**

3 Sample $K - 1$ domains as meta-train \mathcal{D}_{mtr} and the remaining \mathcal{D}_t as meta-test \mathcal{D}_{mte} ;

4 // For simplicity, we denote $\varphi_k(\cdot; W_k), k \neq t$ and $\varphi_g(\cdot; W_g)$ as $\varphi_*(\cdot; W_*)$.

5 **Meta-training:**

6 Sample a mini-batch \mathcal{X}_S from \mathcal{D}_{mtr} .

7 Extract the normal features F and jittered features F' by model with the SJM module:

$$F^* = \{F; F'\} = f_S(\mathcal{X}_S; \Theta);$$

8 Compute meta-train losses by Eq. 20, where the memory $\bar{\mathcal{M}}$ is updated:

$$\mathcal{L}_{mtr} = \mathcal{L}_{all}(\varphi_*(F^*; W_*), F^*);$$

9 Update the original model and meta-train classifiers parameters by:

$$\begin{aligned} \Theta' &\leftarrow \Theta - \alpha \nabla_{\Theta} \mathcal{L}_{mtr}; \\ W_*' &\leftarrow W_* - \alpha \nabla_{W_*} \mathcal{L}_{mtr}; \end{aligned}$$

10 Calculate similarity S with global weight W_g' by Eq. 10 and update the memory \bar{S} ;

11 Calculate domain distances with extracted features F^* by Eq. 14 and update the memory \bar{D} ;

12 **Meta-testing:**

13 Sample a mini-batch \mathcal{X}_T from \mathcal{D}_{mte} .

14 Extract the normal features F by model w/o the SJM module::

$$F = f(\mathcal{X}_T; \Theta');$$

15 Compute meta-test losses w/o the SJM module by Eq. 20:

$$\mathcal{L}_{mte} = \mathcal{L}_{all}(\varphi_t(F; W_t), F)$$

16 Update the meta-test classifier parameters by:

$$W_t' \leftarrow W_t - \beta \nabla_{W_t} \mathcal{L}_{mte};$$

17 **Meta-optimizing**

18 Update the original model parameters Θ by:

$$\Theta \leftarrow \Theta - \gamma (\nabla_{\Theta} \mathcal{L}_{mtr} + \beta \nabla_{\Theta} \mathcal{L}_{mte})$$

19 **end**

IV. EXPERIMENTS

A. Datasets and Evaluation Metrics

Following the previous works [14], [26], [38], [39], we conduct our experiments on public person ReID or Pearson-search datasets, including Market1501 [21], DukeMTMC-reID [40], CUHK02 [41], CUHK03 [42], MSMT17 [43], CUHK-SYSU [44] and four small ReID datasets including PRID [45], GRID [46], VIPeR [47], and iLIDs [48].

Multi-source DG ReID task. On multi-source DG ReID task, we evaluate our methods on large-scale datasets and small-scale datasets, respectively. On large-scale datasets, we train and evaluate on four large datasets, *i.e.* Market-1501, DukeMTMC, CUHK03 and MSMT17. Concretely, we choose one of these four datasets as evaluation dataset and use the remaining three datasets as our training datasets.

Different from evaluation strategies on large datasets, two evaluation protocols (termed as protocol-1 and protocol-2) are adopted on small-scale datasets for the comparison with previous methods. Both two protocols are evaluated on all small-scale datasets (*i.e.* PRID, GRID, VIPeR and iLIDs) and trained on different datasets. Specifically, in protocol-1, we train our model on six large-scale datasets, *i.e.* Market-1501, DukeMTMC, CUHK02, CUHK03, CUHK-SYSU and MSMT17. In protocol-2, we train our methods on four datasets, *i.e.* CUHK03, DukeMTMC, Market-1501 and MSMT17.

Single-source DG ReID task. We have also conduct experiments on single-source ReID DG task. We use two datasets Market-1501 and DukeMTMC in our experiments. In the single-source setting, one of these datasets is used for training and the other one is used for evaluation.

Following the common evaluation metric, the cumulative matching characteristic (CMC) at Rank- k and mean average precision (mAP) are used to evaluate the model's performance on target domains.

B. Implementation Details

We adopt ResNet50 [52] and IBN-ResNet50 [53] pretrained on ImageNet as our backbones, respectively. We add a batch normalization (BN) layer after the global pooling layer to get the ReID feature. A linear classifier is added after BN layer to get classification predictions used for calculating cross-entropy loss and triplet loss [36]. We use the above structure as our baseline. Note that this baseline is different from the strong baseline we proposed. Images are resized to 256×128 , and random cropping and random flipping are utilized as data augmentation. The batch size of each specific domain is set to 128, including 32 identities and 4 images per identity. In training stage, we evenly sample mini-batch from each source domain and combine all these batches as model's input. For optimizing the model, we use Adam optimizer with a weight decay of 5×10^{-4} . The learning rate of meta-train phase and meta-test phase are initialized as 3.5×10^{-4} and are decayed by 0.1 at the 30th and 50th epochs respectively. We train the model on 4 GTX 1080Ti GPUs for 90 epochs. Our SJM module is plugged after the stage-1 of backbone, and the its scale S is set to 4. In addition, the λ in \mathcal{L}_{all} is 0.1.

C. Comparison with State-of-the-Art methods

We compare our methods with the state-of-the-art methods on the multi-source DG ReID task on both large-scale datasets and small-scale datasets. We have also conduct experiments on single-source DG ReID task to demonstrate the effectiveness and generalization ability of our methods.

1) *Results on large ReID datasets under multi-source tasks:* To demonstrate the effectiveness of our method, we compare it with the state-of-the-arts (SOTAs) on the large-scale DG ReID benchmark, including QAConv [49], SNR [14], M3L [25], RaMoE [26] and OSNet [50]. For simplicity, we denote Market-1501 as M, DukeMTMC-reID as D, CUHK03 as C3, MSMT17 as MS.

TABLE I
COMPARISON (%) WITH THE STATE-OF-THE-ARTS DG REID METHODS ON FOUR LARGE-SCALE PERSON REID BENCHMARKS.

Method	Backbone	Reference	D+M+MS→C3		C3+M+MS→D		C3+D+MS→M		C3+D+M→MS		Average	
			mAP	Rank-1	mAP	Rank-1	mAP	Rank-1	mAP	Rank-1	mAP	Rank-1
QAConv [49]	ResNet50	ECCV 2020	21.00	23.50	47.10	66.10	35.60	65.70	7.50	24.30	27.80	44.90
OSNet [50]	OSNet	ICCV 2019	23.30	23.90	47.00	65.20	44.20	72.50	12.60	33.20	31.77	48.70
SNR [14]	ResNet50	CVPR 2020	29.00	29.10	48.30	66.70	48.50	75.20	13.80	35.10	34.90	51.52
M ³ L [25]	ResNet50	CVPR 2021	29.90	30.70	50.30	69.40	48.10	74.50	12.90	33.00	35.30	51.90
MECL [51]	ResNet50	Arxiv	31.50	32.10	53.40	70.00	56.50	88.00	13.30	32.70	38.68	55.70
RaMoE [26]	ResNet50	CVPR 2021	35.50	36.60	56.90	73.60	56.50	82.00	13.50	34.10	40.60	56.57
Baseline	ResNet50	-	32.60	32.90	49.40	65.80	49.90	75.40	9.90	13.50	35.45	46.90
SVIL (Ours)	ResNet50	-	38.50	37.82	58.13	74.78	59.21	82.36	17.06	39.99	43.23	58.74
M ³ L [25]	IBN-ResNet50	CVPR 2021	32.10	33.10	51.10	69.20	50.20	75.90	14.70	36.90	37.02	53.78
MECL [51]	IBN-ResNet50	Arxiv	37.30	38.10	57.20	74.10	60.90	83.20	18.00	41.20	43.35	59.15
SVIL (Ours)	IBN-ResNet50	-	43.22	44.07	61.68	77.33	64.95	86.05	19.85	44.63	47.43	63.02

TABLE II
COMPARISON (%) WITH THE STATE-OF-THE-ARTS DG REID METHODS ON SMALL-SCALE PERSON REID BENCHMARKS.

Method	Source	Target: PRID		Target: GRID		Target: VIPeR		Target: iLIDs		Average	
		mAP	Rank-1	mAP	Rank-1	mAP	Rank-1	mAP	Rank-1	mAP	Rank-1
DIMN [39]		51.95	39.20	41.09	29.28	60.12	51.23	78.39	70.17	57.89	47.47
DualNorm [38]		64.90	60.40	45.70	41.40	58.00	53.90	78.50	74.80	61.78	57.62
MMD-AAE [16]		-	57.20	-	47.40	-	58.40	-	84.80	-	61.95
SNR [14]		66.50	52.10	47.70	40.20	61.30	52.90	89.90	84.10	66.35	57.33
RaMoE [26]		67.30	57.70	54.20	46.80	64.60	56.60	90.20	85.00	69.08	61.52
Baseline		63.77	53.00	50.63	39.00	62.76	53.23	82.34	76.67	64.88	55.47
SVIL (Ours)	C2+C3+D+M+CS	69.39	58.05	56.18	44.20	71.70	63.29	88.97	85.30	71.56	62.63
SNR [14]		60.00	49.00	41.30	30.40	65.00	55.10	91.90	87.00	64.55	55.38
RaMoE [26]		66.80	56.90	53.90	43.40	72.70	63.40	92.30	88.40	71.42	63.02
Baseline		65.18	55.00	52.88	42.60	70.36	62.19	86.03	82.00	68.74	60.45
SVIL (Ours)	C3+D+M+MS	75.28	67.00	56.90	48.00	75.30	67.09	90.03	86.67	74.38	67.19

Following the evaluation protocol for DG ReID in [25], [26], we utilize the leave-one-out protocol to split these four datasets into training/testing datasets. Specifically, we select three datasets as multiple training datasets and the remaining one is used as test dataset. All images in training datasets are utilized for training regardless of train/test splits. The results are shown in Tab I. For the fair of comparison, we provide both results based on ResNet50 and IBN-ResNet50. Under the ResNet50 backbone, our SVIL outperforms our baseline by 9.31%, 8.73%, 5.90% and 7.16% in mAP. Under the ResNet50 backbone, our SVIL outperforms the second best method by 2.71%, 1.23%, 3.00% and 3.26% on M, D, C and MS in mAP respectively. Under the IBN-ResNet50 backbone, our method outperforms the second best method by 4.05%, 4.48%, 5.92% and 1.85% in mAP. The above experiments show our method can achieve state-of-the-art performance on all target domains under different backbones and can outperform baseline by a large margin, which demonstrates the effectiveness and superiority of our method.

2) *Results on small ReID datasets under multi-source tasks:* Following the previous works [14], [26], [38], [39], we adopt the Protocol-1 [39] and Protocol-2 [14] to evaluate our method on four small ReID datasets, respectively. For simplicity, we also denote CUHK02 as C2 and CUHK-SYSU as CS. Under Protocol-1, all images in M+D+C2+C3+CS are utilized for training regardless of train/test splits and the trained network was tested on PRID, GRID, VIPeR and iLIDs, respectively. Our method is higher than other methods on PRID, GRID

and VIPeR datasets under the mAP and Rank-1 evaluation metric. In addition, the proposed method achieves greater improvement than baseline on all datasets. Under Protocol-2, all images in M+D+C3+MS are utilized for training regardless of train/test splits. Our approach outperforms the baseline by a large margin and obtains competitive results compared to SOTAs.

TABLE III
PERFORMANCE (%) COMPARISON WITH THE STATE-OF-THE-ARTS ON THE SINGLE-SOURCE DG-REID TASK.

Method	M→D		D→M	
	mAP	Rank-1	mAP	Rank-1
IBN-ResNet [53]	24.30	43.70	23.50	24.00
OSNet [54]	25.90	44.70	24.00	52.20
OSNet-IBN [54]	27.60	47.90	27.40	57.80
CrossGrad [55]	27.10	48.50	26.30	56.70
QAConv [56]	28.70	48.80	27.20	58.60
L2A-OT [57]	29.20	50.10	30.20	63.80
OSNet-AIN [54]	30.50	52.40	30.60	61.00
SNR [14]	33.60	55.10	33.90	66.70
MetaBIN [15]	33.10	55.20	35.90	69.20
SVIL (Ours)	35.08	56.01	35.05	67.91

3) *Results on large ReID datasets under multi-source tasks:* Since the images of the same dataset come from different cameras, which generally have different styles as mentioned in Sec. I, we divide the single source dataset into K sub-datasets according to the camera information to simulate the setting of multiple source. More specifically, Market1501 [21],

TABLE IV
ABLATIONS STUDIES ON DIFFERENT COMPONENTS OF OUR METHOD.

Backbone	SJM	MAML	Loss	C+D+MS→M		C+M+MS→D	
				mAP	Rank-1	mAP	Rank-1
ResNet50	×	×	\mathcal{L}_{spec}	50.74	77.32	52.64	69.52
ResNet50	✓	×	\mathcal{L}_{spec}	53.76	80.40	53.99	71.50
IBN-ResNet50	×	×	\mathcal{L}_{spec}	58.12	81.80	57.87	73.43
IBN-ResNet50	✓	×	\mathcal{L}_{spec}	58.77	82.36	58.39	73.83
ResNet50	×	✓	\mathcal{L}_{spec}	56.09	80.29	55.74	71.23
ResNet50	✓	✓	\mathcal{L}_{spec}	58.18	82.33	57.26	73.61
IBN-ResNet50	×	✓	\mathcal{L}_{spec}	61.40	83.49	60.24	75.58
IBN-ResNet50	✓	✓	\mathcal{L}_{spec}	63.95	84.77	60.86	76.26
IBN-ResNet50	×	✓	\mathcal{L}_{all}	62.30	83.43	60.72	76.26
IBN-ResNet50	✓	✓	\mathcal{L}_{all}	64.95	86.05	61.68	77.33

TABLE V
ABLATIONS STUDIES OF THE SJM MODULE.

Method	Cross-domain	C+D+MS→M		C+M+MS→D	
		mAP	Rank-1	mAP	Rank-1
SVIL w/o SJM	×	62.30	83.43	60.72	76.26
SVIL w/ SJM	×	64.01	85.34	61.38	76.91
SVIL w/ SJM	✓	64.95	86.05	61.68	77.33

DukeMTMC-reID [40] datasets are divided into 3 subsets according to their cameras, where the camera labels from different subsets do not conflict with each other. Through the division, style variations appear in various sub-datasets. To keep it simple, we discard the domain-specific loss \mathcal{L}_{spec} and preserve the domain-agnostic loss \mathcal{L}_{agno} with the $\lambda = 1$. We then embed our method into the single-source DG-ReID task in the same way as multi-source task. ‘M → D’ in Tab. III indicates that Market1501 is the labeled source training domain and DukeMTMC-reID is the unseen target domain. Experimental results show that our approach achieves competitive performances with SOTAs. However, there is still room for improvement in applying our method to single-domain problems. On the one hand, our division of single source domain is rough. When the subsets are divided only according to the camera label, the identity label space of each subset would overlaps, which is inconsistent with the real multi-source DG-ReID problem. On the other hand, the domain-specific loss is discarded. Both of these factors will prevent our method from achieving better performance. Nonetheless, the comparison in Tab. III also proves that our method can improve the generalization capability of model.

D. Ablation Study

Effectiveness of our SJM module on different backbones.

We plug the SJM module into the two backbones, ResNet-50 [52] and IBN-ResNet-50 [53], and conduct the experiments with different train strategy. As shown in Tab. IV, the results of methods with SJM are all higher than the methods w/o SJM. For instance, mAP/Rank-1 of ResNet50+SJM is 3.02%/3.08% higher than ResNet50, and mAP/Rank-1 of IBN-ResNet50+SJM is 0.65%/0.56% higher than IBN-ResNet50 on M target domain. There is less improvement in IBN-ResNet50 because the Instance Normalization (IN) in IBN-ResNet50 can improve the style-insensitive of the model as well. Its effects

TABLE VI
STUDY ABOUT WHICH STAGE OF IBN-RESNET50 TO PLUG THE SRJ MODULE.

Method	C+D+MS→M		C+M+MS→D	
	mAP	Rank-1	mAP	Rank-1
SVIL w/o SJM	62.30	83.43	60.72	76.26
SJM after stage-0	64.44	85.15	61.16	77.06
SJM after stage-1	64.95	86.05	61.68	77.33
SJM after stage-2	62.90	84.83	59.13	74.46
SJM after stage-3	58.34	81.41	59.01	75.49
SJM after stage-4	50.62	75.00	51.60	70.11

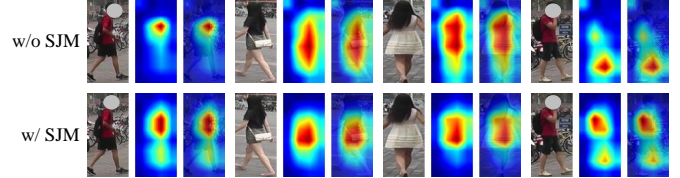


Fig. 3. Visualization of activation maps of different features on method w/o SJM and method w/ SJM. The maps of method with SJM pay more attention to identity-relevant discriminative information, e.g. clothes and bags.

are partially repeated with our SJM module. In addition, the SJM also perform well on the ResNet50/IBN-ResNet50 with MAML. These comparisons confirm the effectiveness of our SJM module.

Effectiveness of our SJM module with MAML. We conducted experiments on two backbones (*i.e.* ResNet50 [52] and IBN-ResNet50 [53]) to prove the effectiveness of the combination of the SJM module and MAML. As shown in Tab. IV, the improvement of SJM module on network with MAML is great than the improvement on network w/o MAML. Take C+D+MS→M as an example, mAP/Rank-1 of IBN-ResNet50+SJM+MAML is 2.55%/1.28% higher than IBN-ResNet50+MAML, and mAP/Rank-1 of IBN-ResNet50+SJM is 0.65%/0.56% higher than IBN-ResNet50. The comparison demonstrates that the combination of the SJM module and MAML would produce a synergy effect and achieves better performance.

Effectiveness of our SJM module on different loss functions. The results in Table IV demonstrate the effectiveness of the SJM module with various losses. For instance, in C+D+MS→M, the improvement of \mathcal{L}_{agno} on IBN-ResNet-50+MAML+ \mathcal{L}_{spec} +SJM is 0.1%/1.37% higher than the improvement on IBN-ResNet-50+MAML+ \mathcal{L}_{spec} on mAP/Rank-1 metrics. This comparison confirms that our SJM module can make cross-domain samples harder.

Effect of different identity relationship modeling. We conduct experiments to confirm the effectiveness of identity relationship modeling in the SJM module. The results in Table V show that only hard identity emphasis can improve the results, and cross-domain identity emphasis can further improve the model performance on the basis.

Effectiveness of which stage to plug the SJM Module. Our SJM module is a plug-and-play module which can be plugged after any stage of the backbone network. We conduct

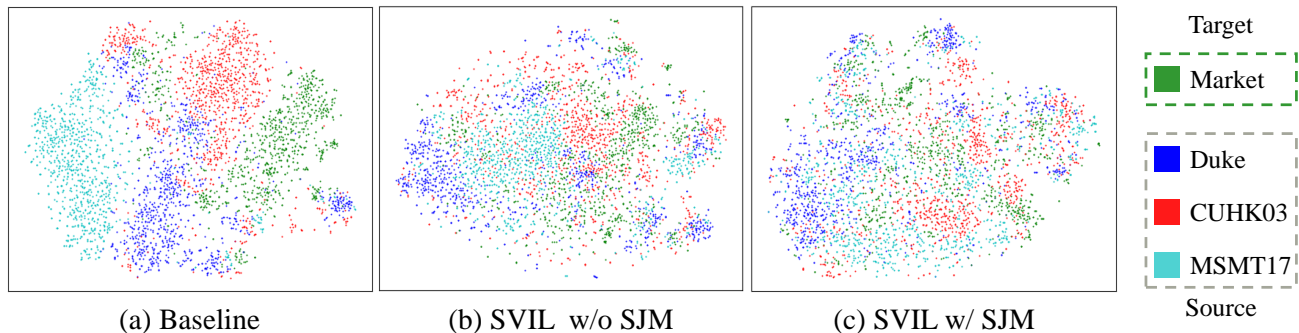


Fig. 4. Visual distributions of four person ReID benchmarks. The distributions are achieved from inference features of (a) Baseline, (b) Our method without SJM module and (c) Our method with SJM module. All of the backbones are ResNet-50 and the dimension of inference features is reduced by t-SNE [58].



Fig. 5. Examples of ranking results on Market1501. The green and red boxes indicate the correct matchings and the wrong matchings, respectively. (a) is the results of baseline, and (b) is the results of our methods.

experiments on the Strong baseline with IBN-ResNet backbone, which has five stages: the stage-0 consists of Conv, BN and Max Pooling layer, and stage-1/2/3/4 are the other four convolutions blocks. We plug the SJM module after different stages to study how different depth will affect the performance of SJM module. Results in Tab. VI shows that our method performs better in shallow stages (0, 1) and worse in deeper stages (2, 3, 4). This phenomenon is because that shallow features contain more low-level features, and the style transformation on them would lose less semantic information.

E. Qualitative Analysis

Visualization of Feature Maps. To better understand the influence of our SJM module, we visualize the intermediate feature maps in the method w/o SJM and method w/ SJM in Fig. 3. Following [14], we obtain each activation map by summarizing the feature maps along channels followed by a

spatial l_2 normalization. We can observe that the maps of our method pay more attention on discriminate areas. For instance, as shown in the 2nd and 3rd columns in the maps, method w/ SJM tends to focus more on bags and skirts, which have some discriminative details. Whereas the focus area of the method w/o SJM is scattered, including part of background and other unimportant areas. These areas may contain more style information. This phenomenon confirms that our SJM module contributes to learning a more style-insensitive and more generalized model.

Visualization of Feature Distributions. In Fig. 4, we visualize the t-SNE [58] distributions of the features on the four benchmarks for baseline and our method. Different colors represent various datasets (*i.e.*, blue, red and cyan denote the source datasets Duke, CUHK03 and MSMT17, respectively; green indicates the target dataset Market1051.). As shown in Fig. 4 (a), we can see the feature distributions of different

datasets on baseline are separately distributed and have visible domain gaps. After adopting our method, these domain gaps are closed a lot. The features of different domains are mixed together.

Visualization of Rank List. Fig. 5 demonstrates 5 pairs of ranking results, *i.e.*, the ranking results of baseline in (a) and the ranking results of our method in (b). We can observe that the wrong matching in baseline generally have similar clothing or background, which share similar styles. Our method can reduce the mismatches caused by style changes. This phenomenon confirms the effectiveness of our approach.

V. CONCLUSIONS

In this paper, we propose a Style Variable and Irrelevant Learning (SVIL) method to eliminate the influence of style factors on the model, thus obtaining a more generalized model. More concretely, we design a Style Random Jitter (SJM) module to enrich the style diversity of source domains. It can prompt the model focus on the identity-relevant information and ignore the style-relevant information. Besides, we organically combine the SJM module with a meta learning algorithm, where the generalization ability of model is improve again. Extensive experiments demonstrate the effectiveness and superiority of our method.

REFERENCES

- [1] Y. Sun, C. Cheng, Y. Zhang, C. Zhang, L. Zheng, Z. Wang, and Y. Wei, "Circle loss: A unified perspective of pair similarity optimization," in *CVPR*, 2020.
- [2] R. Chu, Y. Sun, Y. Li, Z. Liu, C. Zhang, and Y. Wei, "Vehicle re-identification with viewpoint-aware metric learning," in *ICCV*, 2019.
- [3] S. He, H. Luo, P. Wang, F. Wang, H. Li, and W. Jiang, "Transreid: Transformer-based object re-identification," in *ICCV*, 2021.
- [4] L. Wu, C. Shen, and A. van den Hengel, "Personnet: Person re-identification with deep convolutional neural networks," *CoRR*, vol. abs/1601.07255, 2016.
- [5] X. Qian, Y. Fu, Y. Jiang, T. Xiang, and X. Xue, "Multi-scale deep learning architectures for person re-identification," *CoRR*, vol. abs/1709.05165, 2017.
- [6] X. Liu, S. Zhang, Q. Huang, and W. Gao, "RAM: A region-aware deep model for vehicle re-identification," *CoRR*, vol. abs/1806.09283, 2018.
- [7] H. Wang, Y. Wang, Z. Zhou, X. Ji, D. Gong, J. Zhou, Z. Li, and W. Liu, "Cosface: Large margin cosine loss for deep face recognition," in *CVPR*, 2018.
- [8] Y. Ge, D. Chen, and H. Li, "Mutual mean-teaching: Pseudo label refinery for unsupervised domain adaptation on person re-identification," *arXiv preprint arXiv:2001.01526*, 2020.
- [9] L. Song, C. Wang, L. Zhang, B. Du, Q. Zhang, C. Huang, and X. Wang, "Unsupervised domain adaptive re-identification: Theory and practice," *PR*, vol. 102, p. 107173, 2020.
- [10] Y. Fu, Y. Wei, G. Wang, Y. Zhou, H. Shi, and T. S. Huang, "Self-similarity grouping: A simple unsupervised cross domain adaptation approach for person re-identification," in *CVPR*, 2019, pp. 6112–6121.
- [11] D. Kumar, P. Siva, P. Marchwica, and A. Wong, "Unsupervised domain adaptation in person re-id via k-reciprocal clustering and large-scale heterogeneous environment synthesis," in *WACV*, 2020, pp. 2645–2654.
- [12] S. Lin, C.-T. Li, and A. C. Kot, "Multi-domain adversarial feature generalization for person re-identification," *IEEE TIP*, vol. 30, pp. 1596–1607, 2020.
- [13] M. Tamura and T. Murakami, "Augmented hard example mining for generalizable person re-identification," *arXiv preprint arXiv:1910.05280*, 2019.
- [14] X. Jin, C. Lan, W. Zeng, Z. Chen, and L. Zhang, "Style normalization and restitution for generalizable person re-identification," in *CVPR*, 2020, pp. 3143–3152.
- [15] S. Choi, T. Kim, M. Jeong, H. Park, and C. Kim, "Meta batch-instance normalization for generalizable person re-identification," in *CVPR*, 2021, pp. 3425–3435.
- [16] H. Li, S. J. Pan, S. Wang, and A. C. Kot, "Domain generalization with adversarial feature learning," in *CVPR*, 2018, pp. 5400–5409.
- [17] C. Finn, P. Abbeel, and S. Levine, "Model-agnostic meta-learning for fast adaptation of deep networks," in *ICML*, 2017, pp. 1126–1135.
- [18] D. Li, Y. Yang, Y.-Z. Song, and T. M. Hospedales, "Learning to generalize: Meta-learning for domain generalization," in *AAAI*, 2018.
- [19] Y. Balaji, S. Sankaranarayanan, and R. Chellappa, "Metareg: Towards domain generalization using meta-regularization," in *NeurIPS*, 2018.
- [20] E. Ristani, F. Solera, R. S. Zou, R. Cucchiara, and C. Tomasi, "Performance measures and a data set for multi-target, multi-camera tracking," *CoRR*, vol. abs/1609.01775, 2016.
- [21] L. Zheng, L. Shen, L. Tian, S. Wang, J. Wang, and Q. Tian, "Scalable person re-identification: A benchmark," in *ICCV*, 2015, pp. 1116–1124.
- [22] X. Huang and S. Belongie, "Arbitrary style transfer in real-time with adaptive instance normalization," in *ICCV*, 2017, pp. 1501–1510.
- [23] S. Liu, T. Lin, D. He, F. Li, M. Wang, X. Li, Z. Sun, Q. Li, and E. Ding, "Adaattn: Revisit attention mechanism in arbitrary neural style transfer," in *ICCV*, 2021.
- [24] Z. Tang, Y. Gao, Y. Zhu, Z. Zhang, M. Li, and D. Metaxas, "Crossnorm and selfnorm for generalization under distribution shifts," in *ICCV*, 2021.
- [25] Y. Zhao, Z. Zhong, F. Yang, Z. Luo, Y. Lin, S. Li, and N. Sebe, "Learning to generalize unseen domains via memory-based multi-source meta-learning for person re-identification," in *CVPR*, 2021, pp. 6277–6286.
- [26] Y. Dai, X. Li, J. Liu, Z. Tong, and L.-Y. Duan, "Generalizable person re-identification with relevance-aware mixture of experts," in *CVPR*, 2021, pp. 16 145–16 154.
- [27] M. Ye, J. Shen, G. Lin, T. Xiang, L. Shao, and S. C. Hoi, "Deep learning for person re-identification: A survey and outlook," *IEEE TPAMI*, 2021.
- [28] S. D. Khan and H. Ullah, "A survey of advances in vision-based vehicle re-identification," *CVIU*, vol. 182, pp. 50–63, 2019.
- [29] K. Muandet, D. Balduzzi, and B. Schölkopf, "Domain generalization via invariant feature representation," in *ICML*, 2013, pp. 10–18.
- [30] K. Zhou, Y. Yang, Y. Qiao, and T. Xiang, "Domain generalization with mixstyle," *arXiv preprint arXiv:2104.02008*, 2021.
- [31] L. A. Gatys, A. S. Ecker, and M. Bethge, "Image style transfer using convolutional neural networks," in *CVPR*, 2016, pp. 2414–2423.
- [32] C. Li and M. Wand, "Combining markov random fields and convolutional neural networks for image synthesis," in *CVPR*, 2016, pp. 2479–2486.
- [33] Y. Li, N. Wang, J. Liu, and X. Hou, "Demystifying neural style transfer," *arXiv preprint arXiv:1701.01036*, 2017.
- [34] D. Ulyanov, A. Vedaldi, and V. Lempitsky, "Improved texture networks: Maximizing quality and diversity in feed-forward stylization and texture synthesis," in *CVPR*, 2017, pp. 6924–6932.
- [35] V. Dumoulin, J. Shlens, and M. Kudlur, "A learned representation for artistic style," *arXiv preprint arXiv:1610.07629*, 2016.
- [36] A. Hermans, L. Beyer, and B. Leibe, "In defense of the triplet loss for person re-identification," *arXiv preprint arXiv:1703.07737*, 2017.
- [37] F. Wang, X. Xiang, J. Cheng, and A. L. Yuille, "Normface: L_2 hypersphere embedding for face verification," in *ACM MM*, 2017, pp. 1041–1049.
- [38] J. Jia, Q. Ruan, and T. M. Hospedales, "Frustratingly easy person re-identification: Generalizing person re-id in practice," *arXiv preprint arXiv:1905.03422*, 2019.
- [39] J. Song, Y. Yang, Y.-Z. Song, T. Xiang, and T. M. Hospedales, "Generalizable person re-identification by domain-invariant mapping network," in *Proceedings of the IEEE/CVF conference on Computer Vision and Pattern Recognition*, 2019, pp. 719–728.
- [40] Z. Zheng, L. Zheng, and Y. Yang, "Unlabeled samples generated by gan improve the person re-identification baseline in vitro," in *ICCV*, 2017, pp. 3754–3762.
- [41] W. Li and X. Wang, "Locally aligned feature transforms across views," in *CVPR*, 2013, pp. 3594–3601.
- [42] W. Li, R. Zhao, T. Xiao, and X. Wang, "Deepreid: Deep filter pairing neural network for person re-identification," in *CVPR*, 2014, pp. 152–159.
- [43] L. Wei, S. Zhang, W. Gao, and Q. Tian, "Person transfer gan to bridge domain gap for person re-identification," in *CVPR*, 2018, pp. 79–88.
- [44] T. Xiao, S. Li, B. Wang, L. Lin, and X. Wang, "Joint detection and identification feature learning for person search," in *CVPR*, 2017, pp. 3415–3424.
- [45] M. Hirzer, C. Beleznai, P. M. Roth, and H. Bischof, "Person re-identification by descriptive and discriminative classification," in *SCIA*. Springer, 2011, pp. 91–102.
- [46] C. C. Loy, T. Xiang, and S. Gong, "Time-delayed correlation analysis for multi-camera activity understanding," *IJCV*, vol. 90, no. 1, pp. 106–129, 2010.

- [47] D. Gray and H. Tao, "Viewpoint invariant pedestrian recognition with an ensemble of localized features," in *ECCV*. Springer, 2008, pp. 262–275.
- [48] W.-S. Zheng, S. Gong, and T. Xiang, "Associating groups of people." in *BMVC*, vol. 2, 2009, pp. 1–11.
- [49] S. Liao and L. Shao, "Interpretable and generalizable person re-identification with query-adaptive convolution and temporal lifting," in *ECCV*. Springer, 2020, pp. 456–474.
- [50] K. Zhou, Y. Yang, A. Cavallaro, and T. Xiang, "Omni-scale feature learning for person re-identification," in *ICCV*, 2019, pp. 3702–3712.
- [51] S. Yu, F. Zhu, D. Chen, R. Zhao, H. Chen, S. Tang, J. Zhu, and Y. Qiao, "Multiple domain experts collaborative learning: Multi-source domain generalization for person re-identification," *arXiv preprint arXiv:2105.12355*, 2021.
- [52] K. He, X. Zhang, S. Ren, and J. Sun, "Deep residual learning for image recognition," in *CVPR*, 2016, pp. 770–778.
- [53] X. Pan, P. Luo, J. Shi, and X. Tang, "Two at once: Enhancing learning and generalization capacities via ibn-net," in *ECCV*, 2018, pp. 464–479.
- [54] K. Zhou, Y. Yang, A. Cavallaro, and T. Xiang, "Learning generalisable omni-scale representations for person re-identification," *IEEE TPAMI*, vol. PP, 2021.
- [55] S. Shankar, V. Piratla, S. Chakrabarti, S. Chaudhuri, P. Jyothi, and S. Sarawagi, "Generalizing across domains via cross-gradient training," *CoRR*, vol. abs/1804.10745, 2018.
- [56] S. Liao and L. Shao, "Interpretable and generalizable deep image matching with adaptive convolutions," *CoRR*, vol. abs/1904.10424, 2019.
- [57] K. Zhou, Y. Yang, T. M. Hospedales, and T. Xiang, "Learning to generate novel domains for domain generalization," *CoRR*, vol. abs/2007.03304, 2020.
- [58] L. Van der Maaten and G. Hinton, "Visualizing data using t-sne." *JMLR*, vol. 9, no. 11, 2008.